

AD NO. 407453

407 453

DDC FILE COPY

# The A. & M. College of Texas

Department of

OCEANOGRAPHY AND METEOROLOGY



GULF OF MEXICO CLOUD OBSERVATIONS AND  
THE ATMOSPHERIC WATER BUDGET

A Thesis  
By  
RICHARD WESLEY BANKS  
Captain, USAF

May 1963

DDC  
JUN 18 1963  
TISIA B

(4) #5, 1-0

(5) 567 500

(6) GULF OF MEXICO CLOUD OBSERVATIONS AND

THE ATMOSPHERIC WATER BUDGET,

(7) (8) 1-4

(9) Thesis,

(10) By

(11)

RICHARD WESLEY BANKS .

Captain, USAF

Submitted to the Graduate School of the  
Agricultural and Mechanical College of Texas in  
partial fulfillment of the requirements for the degree of

MASTER OF SCIENCE

(12) May 1963, (13) 51 p. (14) - (15) 1-4

(16) 1-1

Major Subject: METEOROLOGY

4 11

GULF OF MEXICO CLOUD OBSERVATIONS AND  
THE ATMOSPHERIC WATER BUDGET

A Thesis

By

RICHARD WESLEY BANKS

Captain, USAF

Approved as to style and content by:

s/ Lymer H. Thompson  
(Chairman of Committee)

s/ Dale F. Leipper  
(Head of Department)

May 1963

## ACKNOWLEDGMENTS

The United States Air Force, acting through the Air Force Institute of Technology, provided the opportunity for me to carry out my graduate program.

Data and other assistance were provided by the Texas A. and M. Research Foundation through Project 285, sponsored by the Cambridge Research Laboratories, U. S. Air Force, under contract No. AF19(604)-8459.

I wish to acknowledge the assistance of my wife, Barbara, whose patience, help, and encouragement made this work possible.

# ABSTRACT

~~This is an initial~~ study <sup>is made</sup> to determine if any detectable relationship existed between the atmospheric water budget and satellite cloud observations over a restricted area. ~~The Gulf of Mexico was selected as the test area.~~ Four consecutive days in July 1961 constituted the time period. Upper air data from nine weather stations, bordering the Gulf of Mexico, were used in the calculations of the water vapor budget. Computations were made of the water vapor storage, water vapor flux, and water vapor balance. The cloud observations were then related to diagrams and graphs of these computations. The large distances between weather stations reduced the value of the computations. The cloudy areas sometimes occurred between stations; therefore the measurements were not always representative of what was happening over the total area. ~~Vertical motion was not considered in this study.~~ The water vapor in the atmosphere had a stream-like structure as it flowed over the Gulf. Clouds were associated with this flow, particularly when it changed direction. ↗

## TABLE OF CONTENTS

	Page
ACKNOWLEDGMENTS.....	iii
ABSTRACT.....	iv
CHAPTER	
I    INTRODUCTION.....	1
General.....	1
Present Status of Knowledge.....	1
Objective and Procedure.....	3
II   DEVELOPMENT OF BASIC RELATIONSHIPS....	6
Water-Vapor Continuity.....	6
Computational Procedure.....	9
Discussion of Error.....	12
III  PRESENTATION AND INTERPRETATION OF RESULTS.....	14
The General Synoptic Picture.....	15
First Day-20 July 1961.....	17
Second Day-21 July 1961.....	25
Third Day-22 July 1961.....	31
Fourth Day-23 July 1961.....	35
Water Vapor Storage, Divergence, Evaporation and Condensation.....	42
IV   SUMMARY AND CONCLUSIONS.....	47
REFERENCES.....	51

# C H A P T E R    I

## INTRODUCTION

The meteorological satellite cloud observations have placed renewed emphasis on the study of clouds in our atmosphere. The satellite provides a "birdseye" view of the clouds never before seen by man. These observations are made by a television camera and are recorded on film at selected ground stations. The area covered by a single picture is roughly that of the Gulf of Mexico. The study of clouds by the use of mathematical laws and measurable data, can be aided greatly by using these pictures.

The use of these pictures to study the relationships between the water budget and the clouds, as observed by the satellite, was largely neglected by previous investigators. Work had been done with the atmospheric water budget in connection with hydrological problems. The methods used in such problems were adapted to this study.

It was recognized that the processes that cause the formation and persistence of cloud masses are many and varied. Moisture is only a part of the total picture. To limit the problem, all factors other than the water budget were neglected in this study.

### Present Status of Knowledge

To date, the atmospheric water budget generally has

been neglected as it relates to cloud observations. Past studies of this budget have been related primarily to hydrology and water flux averages over long periods of time.

Early work by Benton and Estoque (1953) and Starr (1951) used an atmospheric continuity equation for water vapor in broad-scale investigations of water vapor balance over large areas. They were concerned primarily with relating water vapor transfer methods to energy balance considerations.

Franceschini (1961) reduced the area of study and used a continuity equation for the atmospheric water budget in a study of the hydrologic balance of the Gulf of Mexico for a one-year period. He used six pressure levels in the atmosphere to make his computations. His work with water vapor balance gave a relationship between the change in storage of water vapor, water vapor divergence, and the direction of the vertical exchange of water vapor across the lower surface of the volume. If the vertical exchange was positive, evaporation exceeded precipitation. If the value of the exchange was negative, precipitation predominated. When the computations indicated precipitation was predominant instead of evaporation, clouds should be present in the volume.

McKay (1961) used a variation of Franceschini's procedure for computing the atmospheric water budget in his

study of the atmospheric branch of the hydrologic cycle for Texas for a one-year period. He increased the significant levels to sixteen and used monthly averages of data. By making the computations over land, McKay was able to verify the magnitudes of the net vertical exchange of the water vapor across the lower surface of the volume. He compared the computed values with concomitant values of rainfall and evaporation from land stations. He found that the water balance computations generally indicated the correct sign or direction of the net vertical flux. Although the sign was generally correct, the magnitude of the net vertical flux was meaningless. It did not give any indication of how much precipitation or evaporation made up the net flux. He also found that the moisture flowed in concentrated streams. Were these streams the result of using monthly data or can they be observed as daily phenomena, and, if so, are clouds associated with them?

#### Objective and Procedure

The next steps appeared to be to evaluate the atmospheric water budget on a daily basis in as much detail as possible and then to relate the results to the cloud observations, particularly the cloud pictures obtained from the meteorological satellites. In evaluating the water budget, it is convenient to consider a volume fixed

in position. The change in water vapor in such a volume is not only a result of horizontal advection of vapor, but also of other processes including eddy fluxes of vapor, condensation and evaporation of clouds, precipitation, and evaporation from the underlying surface. Not all of these factors can be evaluated readily with available information. However, even though some of the factors are neglected, a cursory evaluation of a simplified daily water budget suggests that moisture streams are quite prominent and are closely related in movement, development, and dissipation to the cloud regions as represented by the satellite television pictures.

The Gulf of Mexico was chosen as the region of interest; the study area is illustrated in Figure 1. The two zones indicated on the map represent volumes within which the continuity equation of water substance was evaluated. Weather station locations are indicated along the boundaries of the zones. Atmospheric soundings from these stations were used as the data sources for the evaluation.

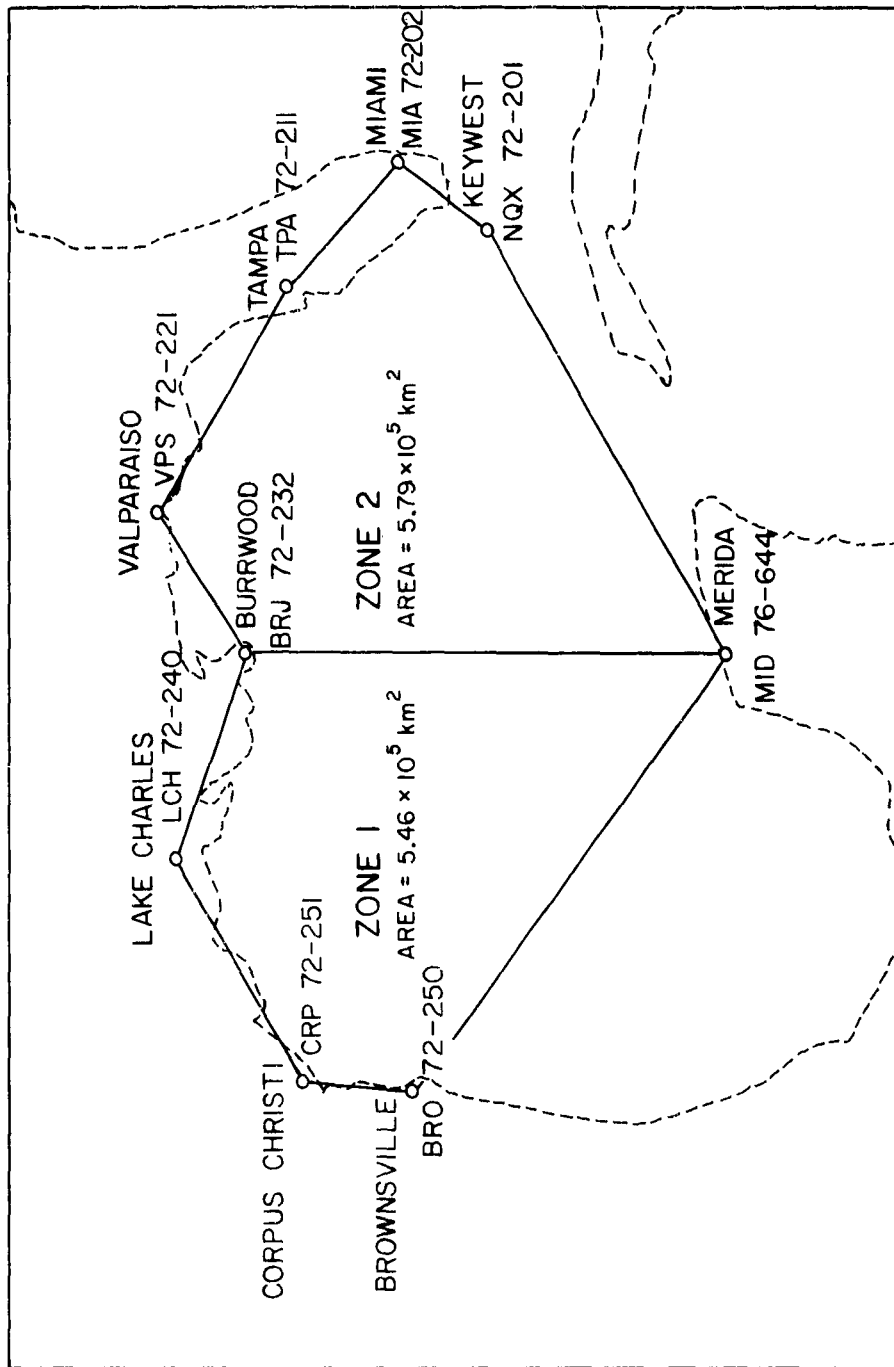


Fig. 1. Location of weather stations used in this study. Name, call letters, and index numbers are indicated for each station. The two zones studied are also indicated.

## C H A P T E R    I I

### DEVELOPMENT OF BASIC RELATIONSHIPS

#### Water Vapor Continuity

The water vapor balance in a volume fixed with respect to the surface of the earth, assuming mass is conserved, can be expressed by a continuity equation for atmospheric water substance. The continuity equation used by Franceschini for a unit volume can be written as

$$\frac{\partial(\rho q)}{\partial t} + \text{div} (\rho q \tilde{V}) + \text{div} \tilde{D} = 0. \quad [1]$$

The mass per unit volume of the water vapor is given by  $\rho q$  where  $\rho$  is air density and  $q$  is specific humidity. The first term gives the local rate of change of water vapor density with time in the unit volume. The second term is the water vapor divergence due to the horizontal wind,  $\tilde{V}$ . The third term combines remaining factors which affect the water vapor budget. These factors include precipitation out of the volume, net condensation or evaporation as clouds form or dissipate, and the vertical transport of water vapor, e.g. evaporation or condensation at the earth-air interface. In application, these factors are difficult to evaluate, compared to the first two terms; the third term was obtained as the residual when the other terms were evaluated and inserted in Equation [1]. Thus, the vector  $\tilde{D}$  is a

combination of the mass transport of water vapor substance across horizontal surfaces, and the mass involved in change of form of water substance.

Equation [1] is more convenient to evaluate if it is converted into another form. The development of the final form will follow the procedure and notations used by Franceschini. The first step is to integrate Equation [1] throughout a unit vertical column of the atmosphere, from the lower surface (sea level) at pressure  $P_0$  to an assumed level of no moisture at pressure  $P$ . The integration of Equation [1] and the assumption of hydrostatic equilibrium yield

$$\frac{\partial w}{\partial t} + \text{div } \widetilde{F} = D_0 , \quad [2]$$

where

$$w = \frac{1}{g} \int_P^{P_0} q dP \quad [3]$$

and

$$\widetilde{F} = \frac{1}{g} \int_P^{P_0} (q\widetilde{V}) dP = \int_P^{P_0} \widetilde{f} dP . \quad [4]$$

Equation [3] gives the mass  $w$  of the water vapor in the total column; this is the "precipitable water." The apparent gravitational force per unit mass is  $g$  and is assumed to be constant at  $980 \text{ dynes gm}^{-1}$ .

The vertically integrated horizontal water vapor flux in the unit column is represented by  $\widetilde{F}$  in Equation [2] and

is defined in Equation [4]. Flux is the rate of flow of the water vapor and has units of mass per length per second. The term  $D_0$  represents the net effect of evaporation and condensation processes; in other words, the phase change.

Equation [2] must be integrated over the area of concern, becoming

$$\frac{\partial W}{\partial t} + \int_A (\text{div } \tilde{F}) dA = (E-C) , \quad [5]$$

where

$$W = \int_A w dA , \quad [6]$$

and

$$(E-C) = \int_A D_0 dA . \quad [7]$$

The earth's curvature is neglected, and the vertical sides of the volume are assumed parallel. The terms  $W$  and  $(E-C)$  are respectively, the total mass of water in vapor phase in the volume and the net change in vapor mass per unit time in the volume due to phase change.  $E$  can be considered as the evaporation and  $C$  as the condensation.

Green's theorem in a plane allows the following transformation.

$$\int_A (\text{div } \tilde{F}) dA = \oint_p F_n dp , \quad [8]$$

where  $F_n$  is the outward directed component of  $\widehat{F}$  normal to the perimeter  $p$ . By substituting Equation [8] into Equation [5] the working equation becomes

$$\frac{\partial W}{\partial t} + \oint_p F_n dp = (E-C) . \quad [9]$$

### Computational Procedure

General. The machine processing methods of McKay were modified slightly and applied to the synoptic upper air data for the stations bordering the Gulf. Each day was computed separately. Variations in temperature, wind and humidity were assumed to be linear between reported pressure levels.

Moisture parameters. The moisture parameters determined from the radiosonde ascents require conversion for use in the equations presented above. Relative humidity, as measured by the radiosonde, was converted to specific humidity using the well-known formulas relating these parameters (Saucier, 1955). The precipitable water was then computed for each station by using Equation [3]. The total precipitable water for each zone was obtained by using the Thiessen polygon method (Linsley, Kohler, and Paulhus, 1949). The changes in precipitable water for each zone were determined for a 24-hour period bounded by the synoptic observation times nearest the satellite picture times.

Transport of water vapor. Instantaneous water vapor fluxes at the surface and for each 50 mb from 1,000 to 300 mb, and the total integrated flux for the column, were computed for each station in the manner described by Franceschini. Each station was considered to be located at a vertex of the polygonal area representing the Gulf as illustrated in Figure 1. The variation of flux between stations was assumed to be linear. To determine the contribution of each station to the total flux of the zone, a base leg was constructed for each station as illustrated in Figure 2.

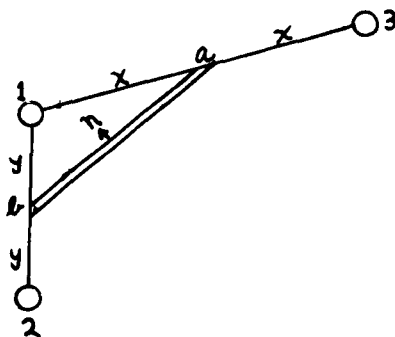


Fig. 2. Diagram defining the base leg used in determining the total flux. The base leg for Station 1 extends from a to b and has outward directed normal n. Stations 2 and 3 are the adjacent stations.

This base leg was determined by connecting the mid-points of the boundary lines joining the station to its two adjacent stations. The flux normal to the boundary from b

to Station 1 to a is equal to the flux normal to the base leg. The orientation of the base leg determines the direction taken as normal to the vertical surface for that station. The length of the base leg represents the length of the boundary represented by the station. The flux normal to the base leg at a selected level is given by

$$f_n = \frac{1}{g} qV_n \quad [10]$$

and the tangential flux is

$$f_t = \frac{1}{g} qV_t , \quad [11]$$

where  $V_n$  is the component of observed wind, normal to the base leg and  $V_t$  is the component tangential to this leg. These winds are determined by

$$V_n = V \cos (\alpha - \beta) \quad [12]$$

and

$$V_t = V \sin (\alpha - \beta) \quad [13]$$

where  $V$  is the observed wind in meters per second,  $\alpha$  the direction, measured clockwise from north, of the unit normal directed outward from the base leg, and  $\beta$  is the reported wind direction. The flux units are in  $\text{gm sec}^{-1}\text{m}^{-1}\text{mb}^{-1}$ .

Vertically integrated flux. The vertically integrated flux was computed in the manner described by McKay. Equations [4], [10], and [11], and the trapezoidal rule, as described by Milne (1953), were used.

Water-vapor flux divergence. It was assumed that the vertically integrated flux  $F$ , varies linearly between stations. Then, according to Franceschini, the net water-vapor divergence ( $\text{gm sec}^{-1}$ ) is

$$\int_A \text{Div } \tilde{F} \, dA = \sum_{i=1}^j (z_i \tilde{n}_i \cdot \tilde{F}_i) \quad [14]$$

where  $\tilde{F}_i$  is the computed value of vertically integrated flux for station  $i$ ,  $z_i$  is the length of the base leg at station  $i$ , and  $\tilde{n}_i$  is the outward-directed unit normal for station  $i$ . The contributions of  $j$  stations located on the zone boundary are summed. This sum is the water-vapor flux divergence for the zone.

#### Discussion of Error

An Air Weather Service study (Anon., 1955) gives the total error in relative humidity and temperature measurements measured by radiosonde as about  $\pm 5$  per cent. The error in measurement of the wind vector is more complicated due to the difference in the variation of the vector with height. According to studies by Ellsaesser (1960) and by Sawyer (1962), a  $\pm 7$  per cent vector error is to be expected over the Gulf of Mexico.

The variation of flux between stations was assumed to be linear. The evaluation of Equation [9] depends

upon this assumption. An estimate of the error resulting from this assumption can be obtained by omission of data for a weather station. This changes the shape of the zone. In cases where the flow did approximate linear conditions a  $\pm 10$  per cent error appeared probable for the computed values in Equation [9]. When a strong concentrated flow was moving through the zone, a probable error of  $\pm 70$  per cent occurred in the results of this equation.

The flux values computed for each station are unaffected by the assumption of linear flow. They then contain only the error of  $\pm 12$  per cent due to error in data measurements. This fact makes the charts using these data the most valuable part of the study.

The satellite observations and upper-air data measurements were made at different times. The cloud pictures were generally taken two to four hours after the upper air data were measured. Assuming a linear change, this time difference introduces a 10 to 15 per cent error in vapor budget computations.

### C H A P T E R    III

#### PRESENTATION AND INTERPRETATION OF RESULTS

This study was conducted by using four sets of satellite cloud observations taken on four consecutive days, 20 through 23 July 1961. The upper air data are taken twice a day at 12 GCT and 00 GCT. As this time is at the beginning and ending of the daylight period over the Gulf, the existing light is not enough for good cloud observations. The cloud observations are made during daylight hours, between 12 GCT and 00 GCT. The upper-air data collected nearest the cloud observation time were used to calculate the water budget. A given "time period" includes both the time of the cloud observation and its associated data. As there is just one cloud observation and its associated data per day these time periods are labeled with the day of occurrence.

The synoptic conditions of the four days studied are first summarized. Each day is then considered individually. The specific synoptic pattern is examined briefly and related to the corresponding TIROS cloud pictures. The results of the evaluation of the water budget for that day are then presented, with emphasis placed on the vertical distribution of water vapor flux and the vertically integrated water vapor flux. Finally, the entire four

days are summarized using the water vapor balance as computed by Equation [9].

The computation of Equation [9] required a decision on how the change in atmospheric storage should be computed. The method suggested by Franceschini of averaging the difference between the precipitable water in storage over the zones for the preceding and following time period did not produce the desired results. The satellite cloud observation on 22 July, illustrated in Figure 11, shows that Zone Two has very few clouds. It was felt that if Equation [9] were to indicate that evaporation exceeded condensation, it should do so on a nearly clear day. The only way this was achieved was to use the divergence computed from the upper air data associated with the cloud picture. The change in storage term was computed assuming a linear change over the previous twenty-four hours. The poor results from the use of averaged terms tends to agree with the cloud pictures over the four days, in that each day has its own individual characteristics and is not an average condition of the preceding and following days.

#### The General Synoptic Picture

The western part of the Bermuda High exerts dominant control over the weather of the Gulf of Mexico during the summer months. Such was the case from the 20th to the 23rd

of July in 1961. The long west-east axis of the high at the surface was fairly close to the middle of the Gulf. This led to generally southeasterly flow over the southern parts and southerly or southwesterly flow over the northern parts of the Gulf. The tilt of the high axis toward the warmer air to the south, though slight, was sufficient to result in generally southwesterly flow at higher tropospheric levels.

This general pattern was complicated by the presence of an easterly wave which moved from the Caribbean Sea across the Yucatan Peninsula into the Gulf during the early part of the period. At the same time, a weak trough in the middle tropospheric westerlies moved across the northern part of the Gulf. Both troughs reached approximately the same longitude, that of the western Gulf, at the beginning of the study period. Superposition resulted in apparent deepening, and the resultant impulse then moved eastward or east-northeastward and gradually weakened, crossing the Florida Peninsula about the 23rd.

At the same time, Hurricane Anna, which had formed several days earlier, was moving westward just north of the north coast of South America. This storm arrived in the western Caribbean Sea about the 23rd. While a well developed tropical storm, Anna appeared to play an unimportant role as far as the conditions discussed in this paper are concerned. The storm did seem to have some effect on the

cloudiness in the southeastern part of the Gulf about the 23rd.

#### First Day-20 July 1961

The cloud pictures. The clouds pictured by the TIROS photographs of the 20th (Figure 3) are representative of the time of merging of the easterly wave and the westerly trough. This picture shows a large mass of clouds extending across the boundary into Zone One between Merida (MID) and Brownsville (BRO). The cloud mass broke into two smaller patches as it curved eastward between MID and Burrwood (BRJ) into Zone Two. The eastern section of Zone Two does not show in the picture but general indications from a picture taken from over the Caribbean Sea placed a third narrow cloud mass in Zone Two extending in a west-east direction over Tampa (TPA). These cloud masses appeared to be part of a well organized group, as few clouds appear elsewhere in the picture.

The cloud system was generally crossing the zonal boundaries at points where measurements were not made. The data measured at the stations were assumed to be representative of what was happening along the boundary. This conflict between the size of the cloud system and the distance between measuring stations was resolved by adjusting the analysis of the flux isopleths between

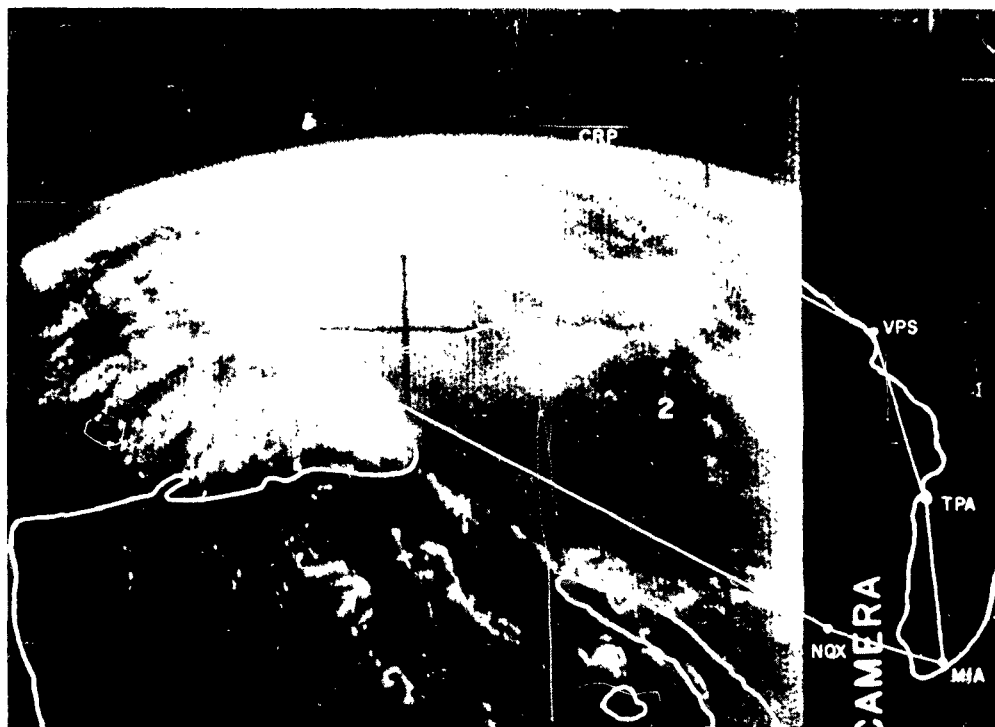


Fig. 3. TIROS III satellite cloud observation for 1627 GCT, 20 July 1961. (Orbit 119 Frame 12T). Coastlines and zone boundaries are superposed on the cloud picture.

stations in some cases to account for what appeared to be occurring.

The vertical distribution of flux. Figures 4 and 5 represent the vertical distribution of the water vapor flux normal to the base legs of the two zones of Figure 1. These figures of the flux were constructed by plotting the magnitude of the normal vector at each level for which it was computed, along the vertical over the station. Assuming linear change between stations, except where evidence such as the cloud pictures suggests otherwise, isopleths indicating the magnitude of the flux were drawn for every  $500 \text{ gm sec}^{-1} \text{ m}^{-1} \text{ mb}^{-1}$  of flux.

These figures show centers of maximum inflow and outflow of moisture into the zones. These concentrated areas of moisture flux may be defined as a stream-type flow. The distortion of the stream in the figures is influenced by the angle at which the flow intersects the direction of the base leg line. A good illustration of this type of flow is in Figure 5, which illustrates a stream crossing approximately perpendicular to the boundary at Tampa (TPA). The center of the moisture is at approximately 950 mb and extends upward toward 600 mb. In general, stream flow was centered at 900 mb and dropped off rapidly above 750 mb. Flux values above 700 mb were generally about ten per cent of those at the lower levels.

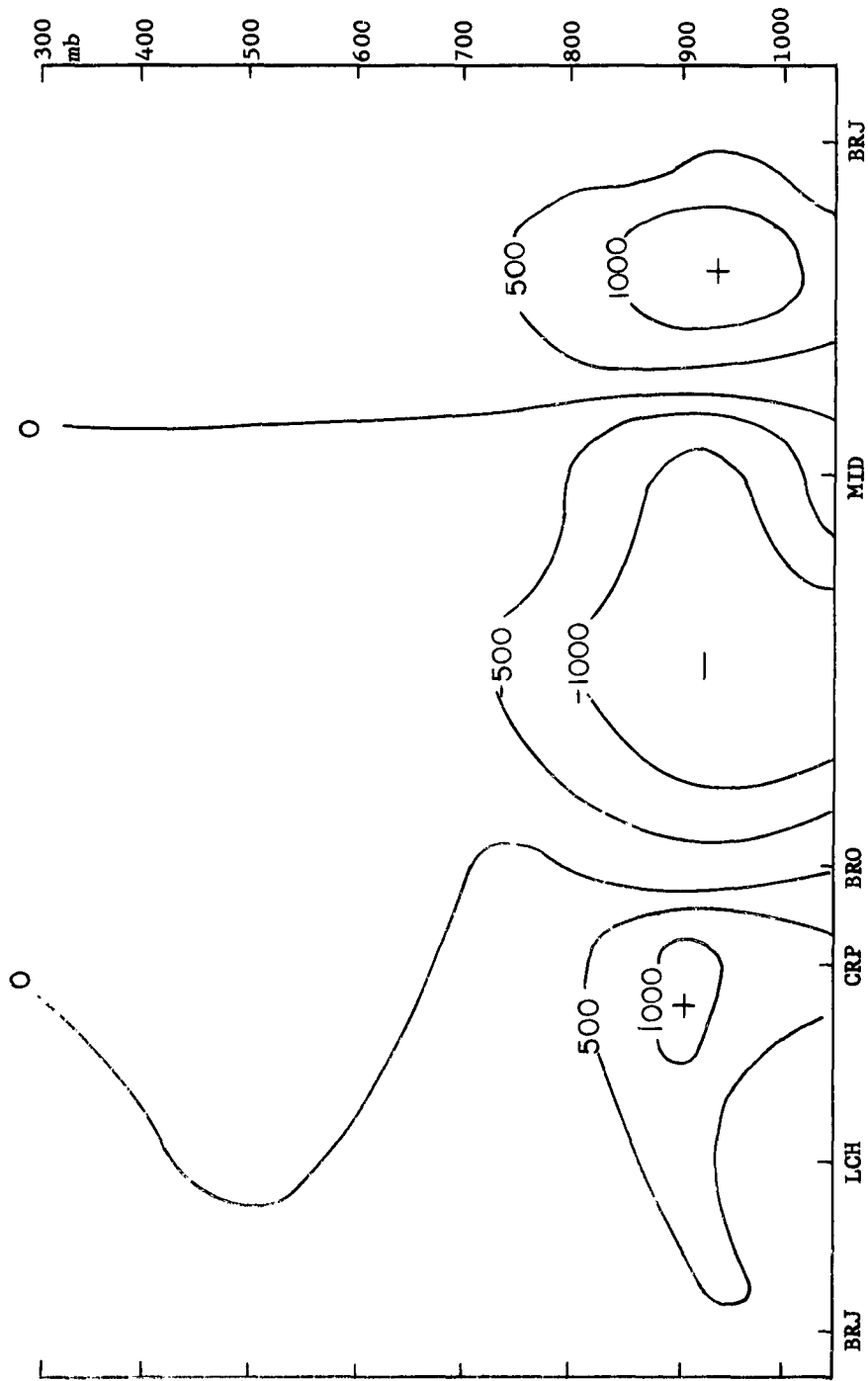


Fig. 4. Vertical distribution of flux of water vapor normal to the base legs of Zone One at 1200 GCT, 20 July 1961. Flux is in  $\text{gm sec}^{-1} \text{m}^{-1} \text{mb}^{-1}$ . Negative flux is inward and positive flux is outward.

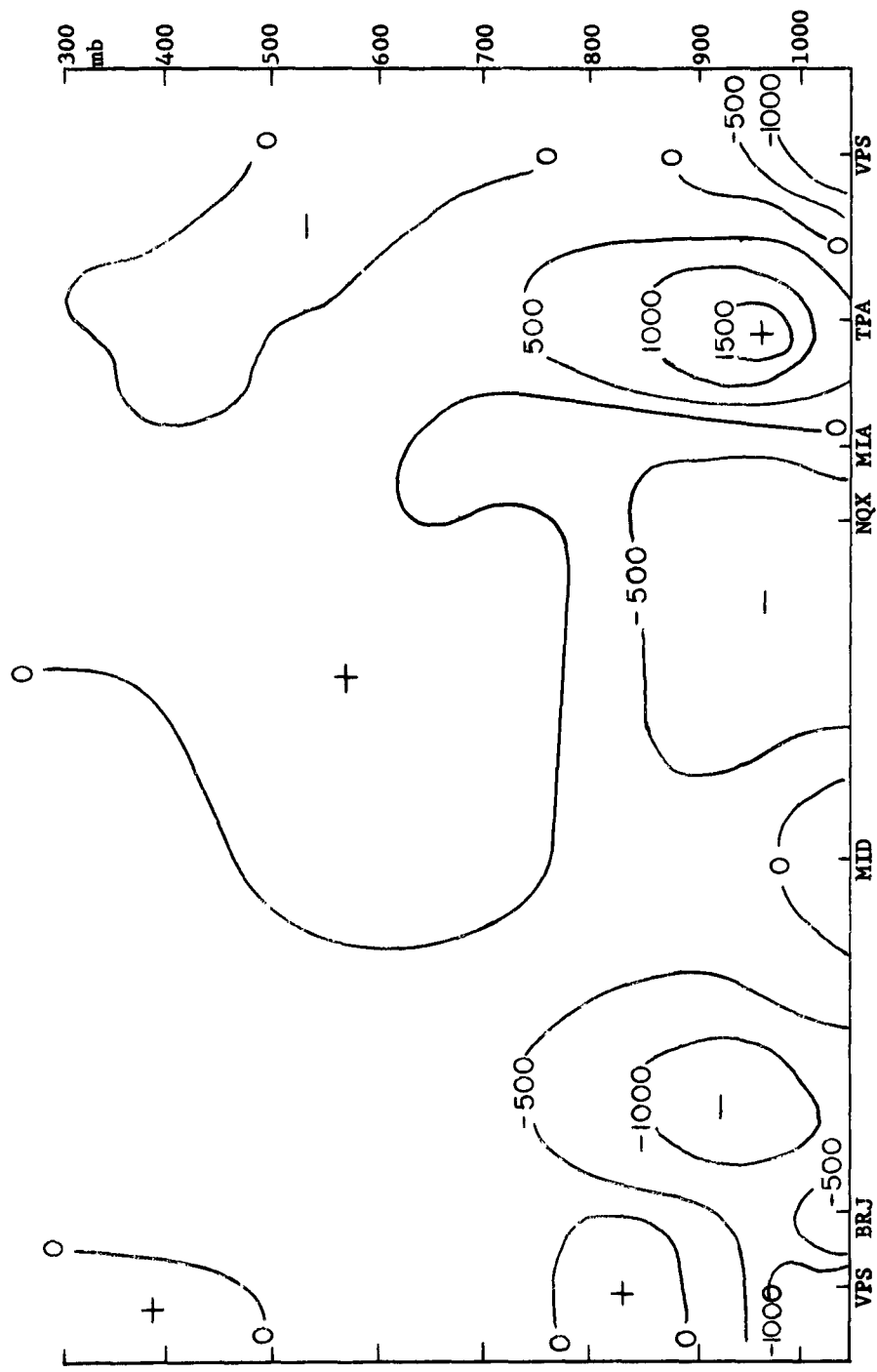


Fig. 5. Vertical distribution of flux of water vapor normal to the base legs of Zone Two at 1200 GCT, 20 July 1961. Flux is in  $\text{gm sec}^{-1} \text{m}^{-1} \text{mb}^{-1}$ . Negative flux is inward and positive flux is outward.

The vertically integrated flux. Another view of the flux through the zones can be obtained by vertically integrating the fluxes of the different layers and placing the results on a map of the area. Such a map for the fluxes of the 20th is represented in Figure 6. The maps are constructed by first adding the vertically integrated tangential and normal flux vectorally at each station. The resulting vector is plotted at the station. Isopleths are drawn for the magnitude of the vectors for intervals of  $50 \text{ kgm sec}^{-1} \text{m}^{-1}$ . The triple-lined arrows give an estimated location of the region of maximum flux.

The primary feature illustrated in Figure 6 is the maximum of the water vapor flux in the eastern part of Zone Two; the flux was quite intense in the vicinity of TPA. This flow can be quite concentrated and requires close spacing of data points for detection. If TPA had been omitted as a measuring point in Zone Two, this strong stream might have been undetected. The cloud pictures, however, support the analysis showing the region of high flux values. The possible variation in flux with distance is shown by the doubling of magnitude and the change in direction by 90 degrees between MIA and TPA. Although this flux tends to indicate the heavier low level flow it is possible to visualize a low level flux in one direction being cancelled out in the computations by a strong higher level flux in the opposite direction.

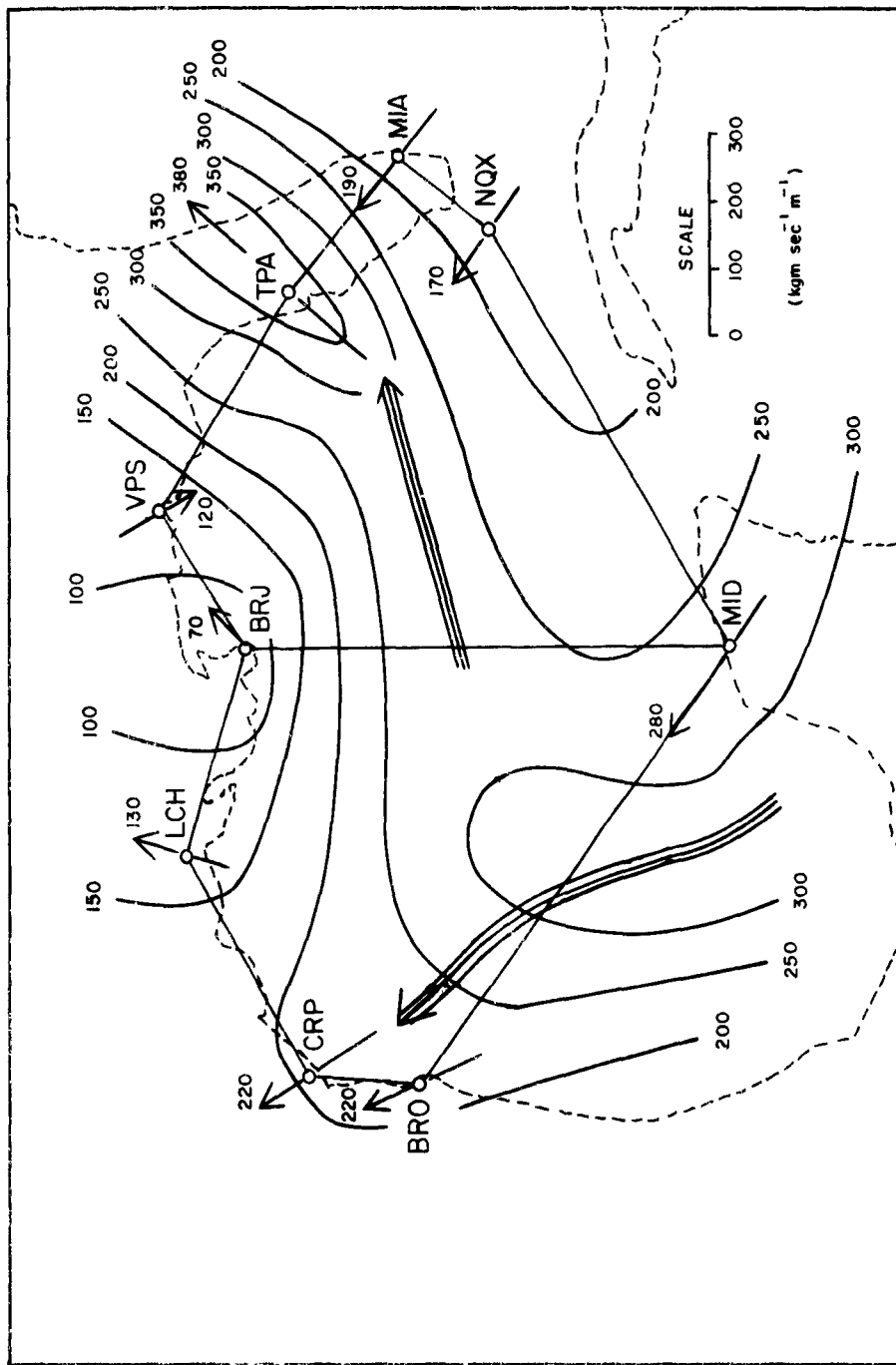


Fig. 6. Vertically integrated flux of water vapor for 1200 GMT, 20 July 1961. Lengths of the vectors are proportional to the magnitude of the flux.

The presence of the stream in Zone One was harder to determine. Figure 6 indicated the stream entering Zone One between MID and BRJ. The area of high flux values was located by using the position of the clouds in Zone One. The integrated flux vectors and the vertical distribution flux chart (Figure 4) did indicate a slight stream flow continuing from south of MID toward CRP.

The location of the stream entering Zone One was partially verified by other evidence. Analysis of the upper air data at MID, on the Yucatan Peninsula, over the previous two days, revealed that an easterly wave had moved through the region. The cloud mass west of MID appeared to be associated with this easterly wave. The flux in the vicinity of the cloud mass was assumed to be similar to that over MID at the time the wave passed MID. The curving of the cloud mass into Zone Two between MID and BRJ was associated with the northeastward extension of the merged troughs. The moist southerly flow in the easterly wave in Zone One was picked up by the westerly winds in the northern part of the trough and carried eastward over TPA. It seems that conditions associated with the easterly wave and the trough provided the vertical motion needed for the cloud development.

## Second Day-21 July 1961

The cloud pictures. By the 21st, the main cloud masses over the southern Gulf had moved northwestward and the individual elements somewhat eastward (compare Figures 3 and 7). At the same time, the overall amount of cloud appeared to have decreased, though this conclusion is admittedly subjective. These changes are associated with the westward drift of the easterly wave, eastward drift of the trough, and gradual dissipation of the merged trough systems. The clouds appeared to be organized into two groups, one in the northwestern part of Zone One and the other in the eastern section of Zone Two.

The vertical distribution of flux. The vertical distribution of the flux normal to the zonal base legs for this day are illustrated in Figures 8 and 9. The flux in Zone One showed inflow from the south and an outflow through the northern boundary. The flow in Zone Two was concentrated in the eastern side with inflow from the south and outflow through the north side.

Zone One (Figure 8) indicated an increase over the previous day in the inflow over MID through the southern boundary (compare Figure 4). This increased inflow was also followed by an increase in the outflow in the northern and western boundaries. The inflow occurred at a higher



Fig. 7. TIROS III satellite cloud observation for 1544 GCI, 21 July 1961. (Orbit 133 Frame 31T). Coastlines and zone boundaries are superposed on the cloud picture.

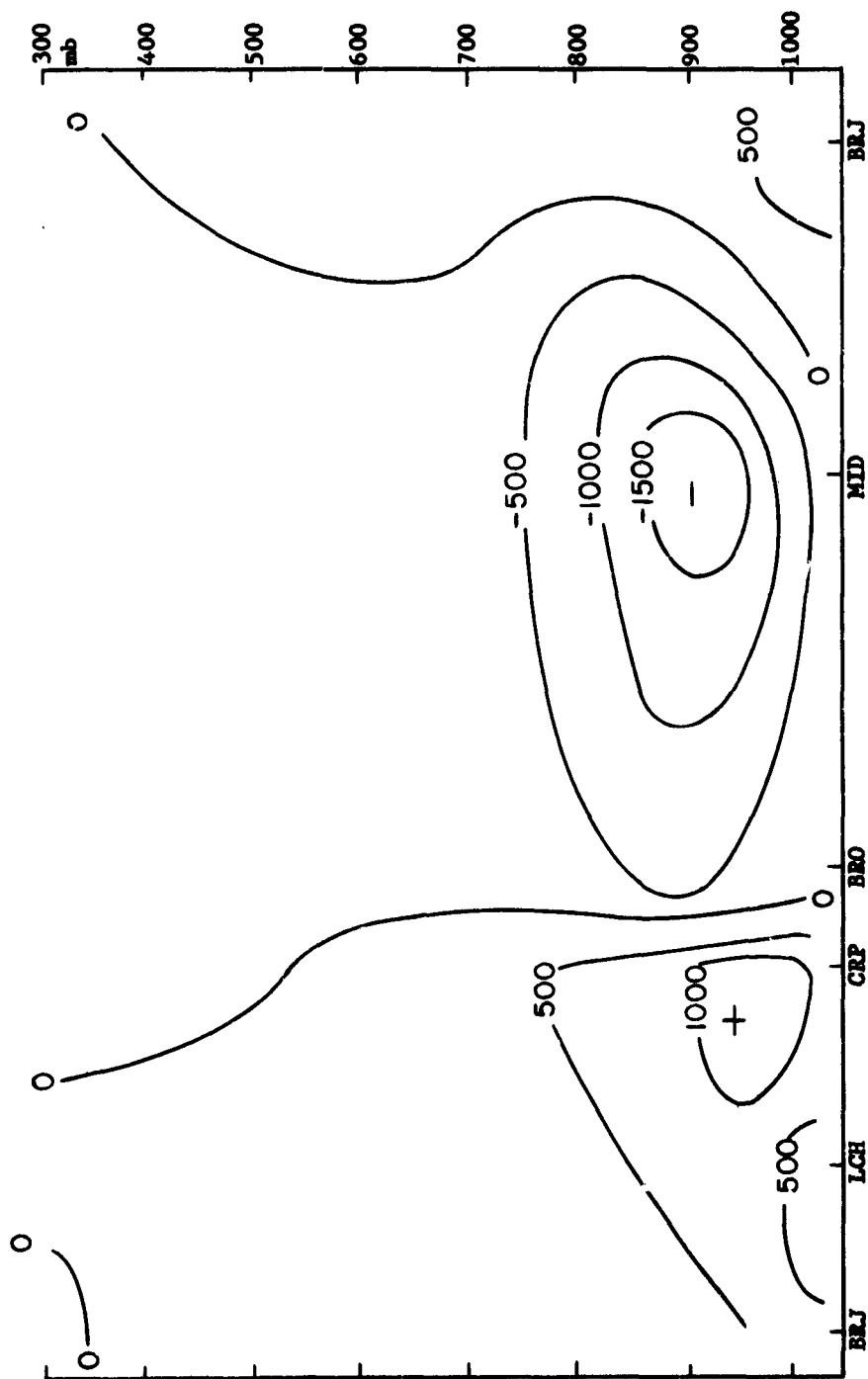


Fig. 8. Vertical distribution of flux of water vapor normal to the base legs of Zone One at 1200 GCT, 21 July 1961. Flux is in  $\text{gm sec}^{-1}\text{m}^{-1}\text{mb}^{-1}$ . Negative flux is inward and positive flux is outward.

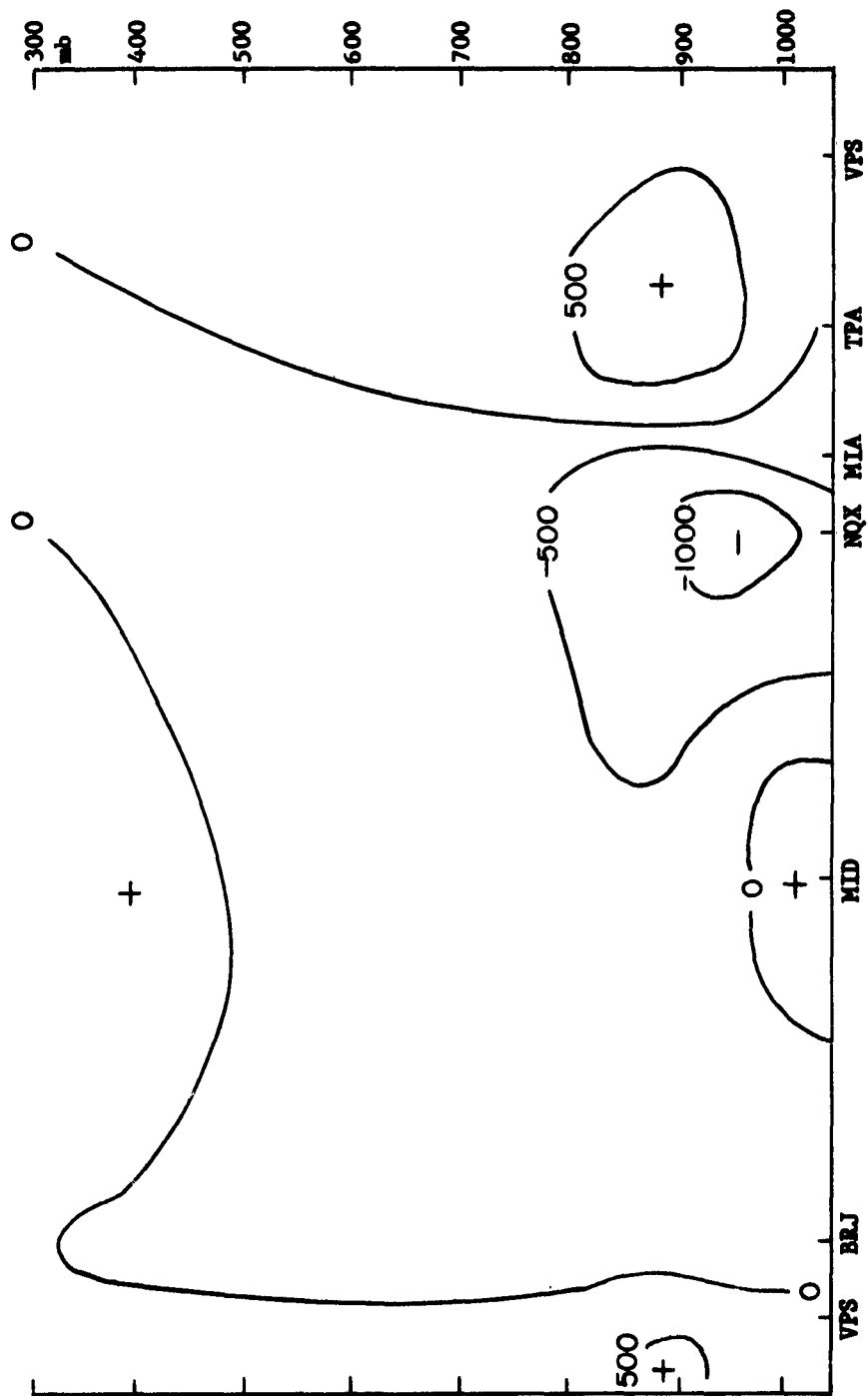


Fig. 9. Vertical distribution of flux of water vapor normal to the base legs of Zone Two at 1200 GCT, 21 July 1961. Flux is in  $\text{gm sec}^{-1}\text{m}^{-1}\text{mb}^{-1}$ . Negative flux is inward and positive flux is outward.

level than the outflow. This is due partly to the more southerly direction of the winds near 900 mb while those at the surface are more easterly.

Zone Two (Figure 9) showed an increase in the inflow from the south over Key West (NQX) and the dissipation of the inflow from the west on the previous day (compare Figure 5). The strong outflow of the previous day near TPA had changed to a less intense outflow between TPA and Valparaiso (VPS). An interesting feature of Figure 9 is the increase in height of the stream as it passed from NQX to TPA. This change did not appear to be a result of a difference in wind component but possibly to an actual lifting of the moisture stream.

The vertically integrated flux. The vertically integrated flux for this day (Figure 10) showed considerable change from the previous day (Figure 6). The flux from the southwest through both zones was replaced by an increased flux across the southern part of Zone One and a slight indication of a stream flowing from the south through the eastern part of Zone Two (based in part on calculations for stations south of Cuba). The flux in the southern and western part of Zone One had almost doubled over the previous day.

The clouds again appeared to be associated with the moisture streams. The more intense area of clouds in

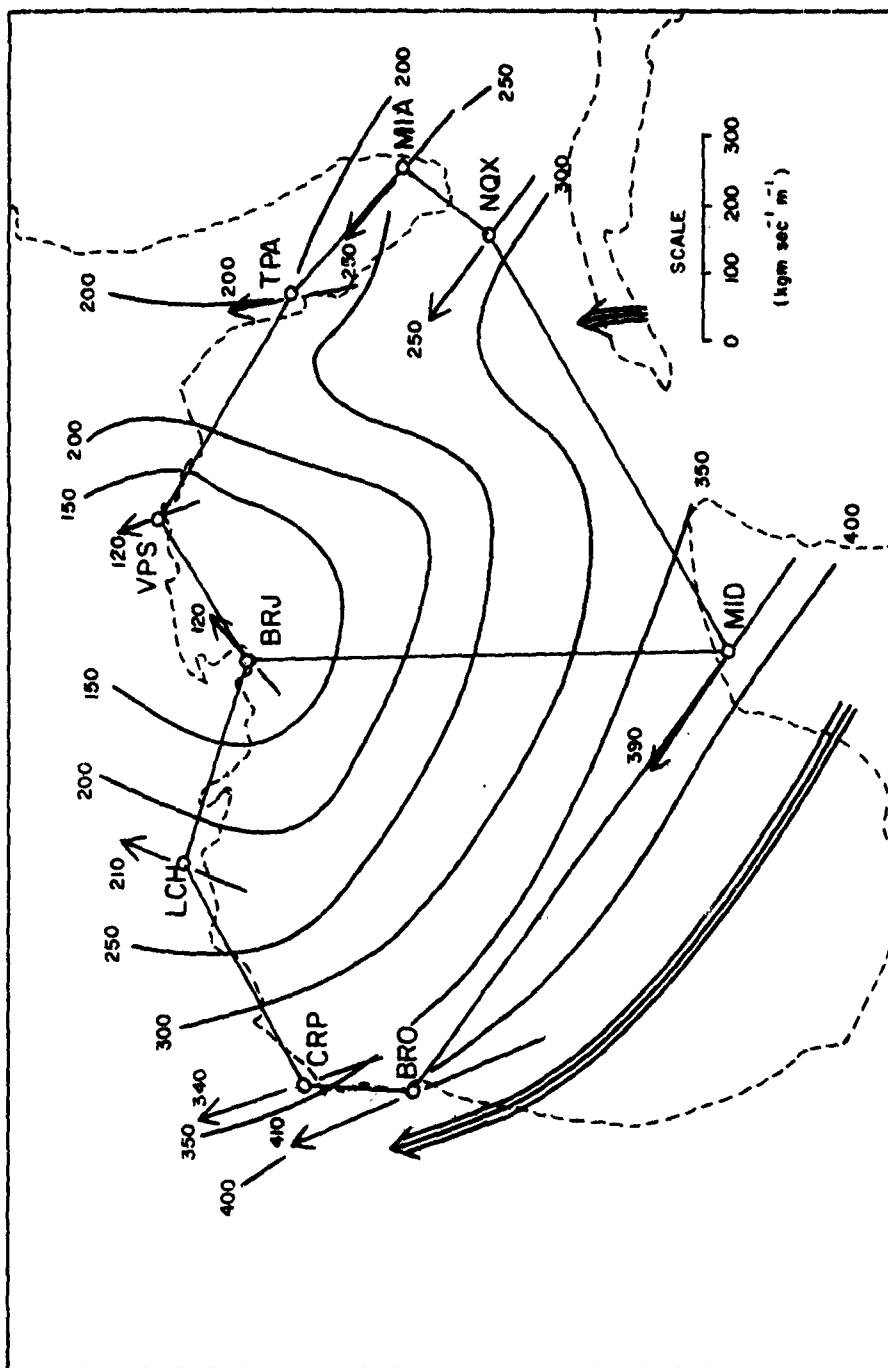


Fig. 10. Vertically integrated flux of water vapor for 1200 GMT, 21 July 1961. Lengths of the vectors are proportional to the magnitude of the flux.

Zone One was located in the western section where the moisture stream south of the zone curved more northward. In Zone Two the clouds were located in conjunction with the moisture stream.

### Third Day-22 July 1961

The cloud pictures. On the 22nd, the clouds in the northern Gulf increased with the main cloud mass located in the northeast corner of Zone One (Figure 11). The overall cloud amount appeared to have decreased slightly from the previous day. Southerly flow was predominant from the surface to 500 mb throughout Zone One. Some cloud streaks in Zone One were aligned parallel to this flow. In Zone Two a weak trough was just approaching western Florida. The clouds along the northern boundary of Zone Two appeared to be associated with this trough.

The vertical distribution of flux. The vertical distribution of flux (Figure 12) along the boundary of Zone One showed an increase in the flux over the previous days. The inflow through the southern and eastern sides increased in intensity, in width, and particularly in height. The height increased by 100 mb at MID and by 200 mb at BRO. The increased inflow was matched by an increase in outflow along the northwestern boundary. In Zone Two (Figure 13) the inflow remained in about the



Fig. 11. TIROS III satellite cloud observation 1510 GCT, 22 July 1961. (Orbit 147 Frame 19T). Coastlines and zone boundaries are superposed on the cloud picture.

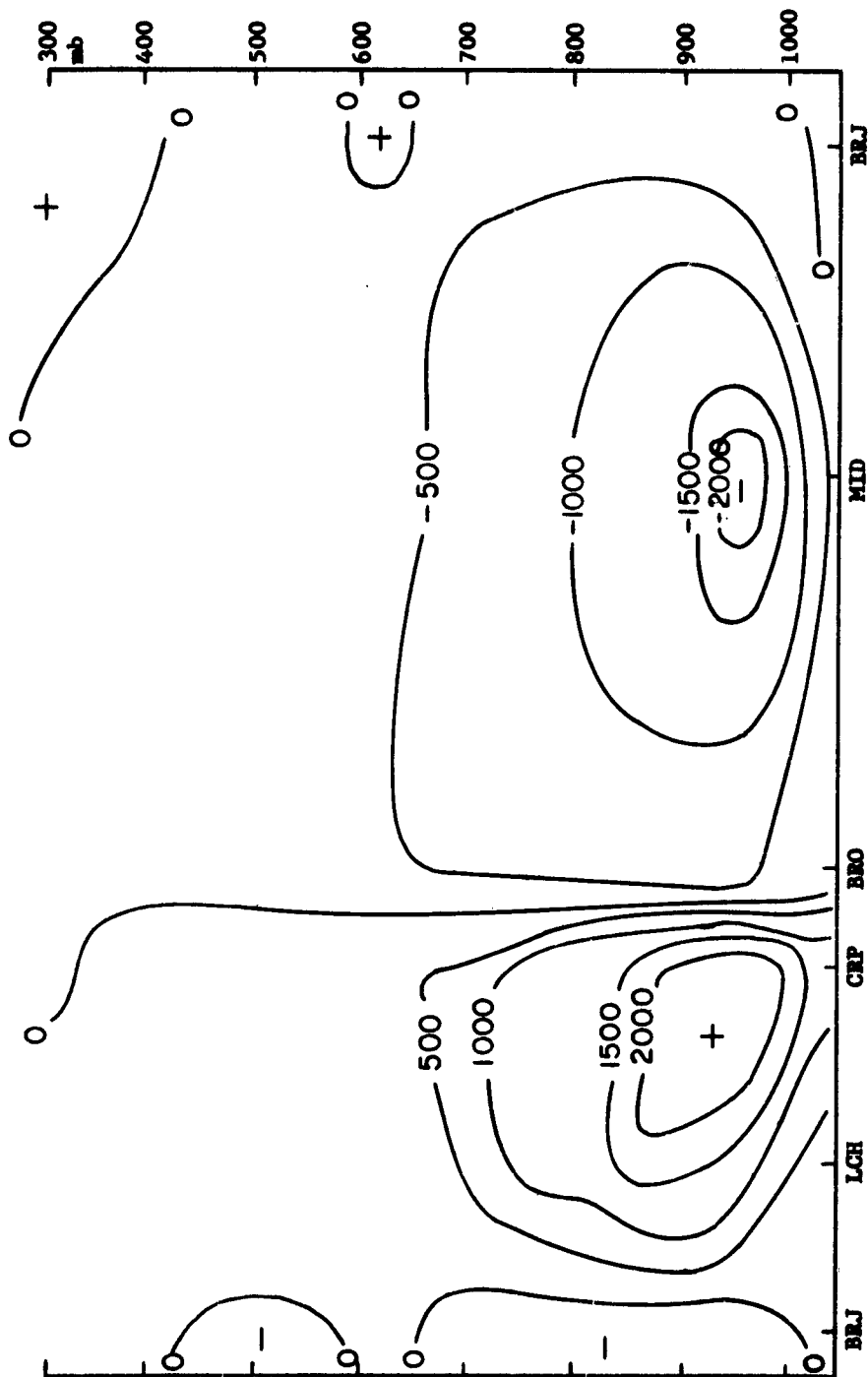


Fig. 12. Vertical distribution of flux of water vapor normal to the base legs of Zone One at 1200 GCT, 22 July 1961. Flux is in  $\text{gm sec}^{-1} \text{m}^{-1} \text{mb}^{-1}$ . Negative flux is inward and positive flux is outward.

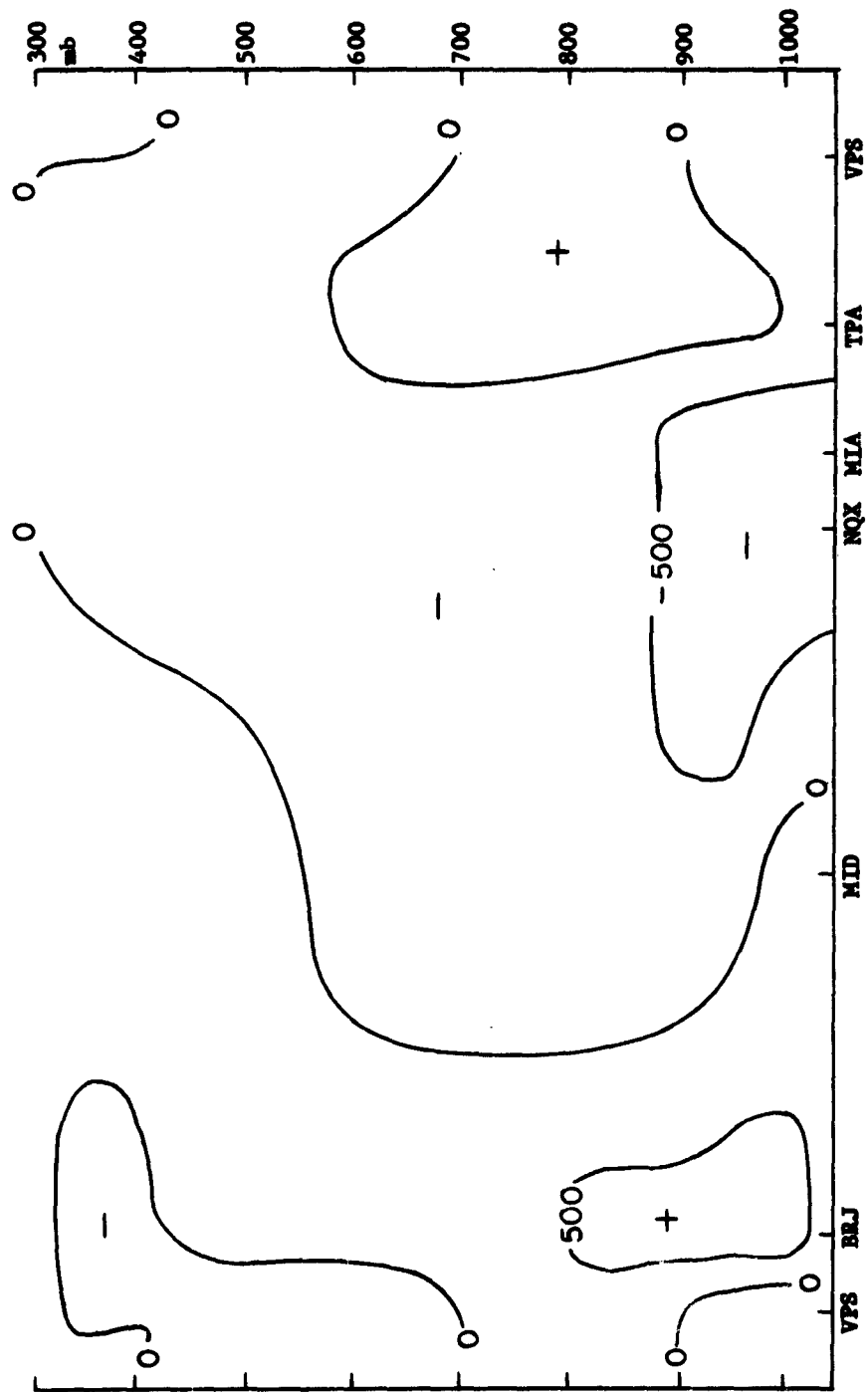


Fig. 13. Vertical distribution of flux of water vapor normal to the base legs of Zone Two at 1200 GMT, 22 July 1961. Flux is in  $\text{gm sec}^{-1} \text{m}^{-1} \text{mb}^{-1}$ . Negative flux is inward and positive flux is outward.

same location over the southeast corner of the zone, but the more concentrated outflow changed from near TPA to BRJ. The predominant cloud mass was also located near BRJ.

The vertically integrated flux. This flux, as illustrated in Figure 14, had the least distortion of the three days. The hump in the eastern part of Zone Two of the previous day was gone. The pattern was generally characterized by an increase in the flux along the southwestern part of Zone One with the intensity decreasing northeastward through the two zones.

The main cloud area was located in the region where the flux gradient appeared to be compressed between LCH and VPS. Cloud streaks were observed in Zone One where the more intense flux, relative to Zone Two, was curving more northward.

#### Fourth Day-23 July 1961

The cloud pictures. The only zone photographed by the satellite on this day was Zone Two (Figure 15). A slight southeasterly motion of the clouds moved them more into the northern part of Zone Two. The trough that had been just west of Florida had moved eastward and was replaced by a ridge aloft. Another westerly trough was moving into Zone One. Some cloud streaks were noted between MIA and MID.

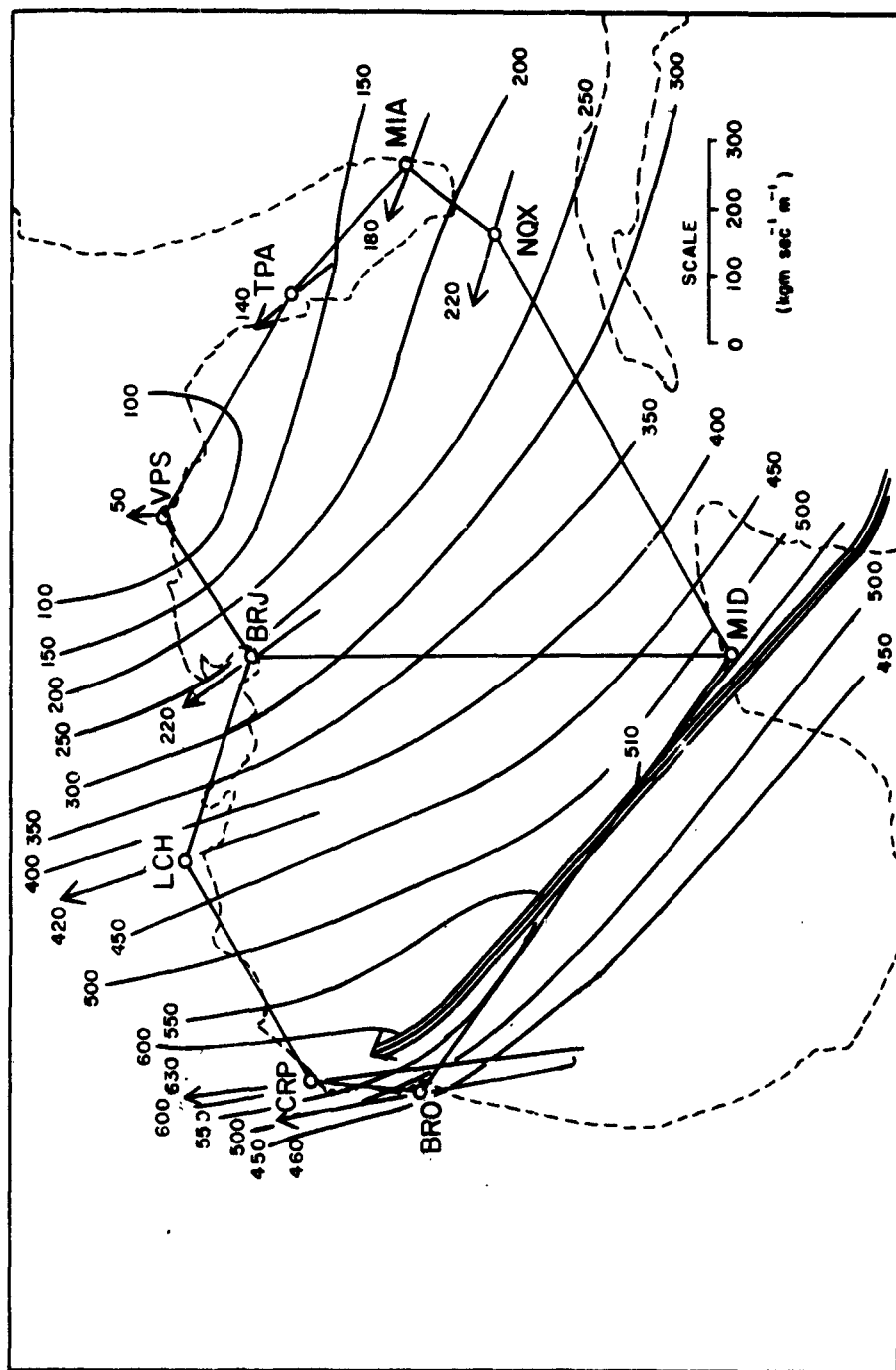


Fig. 14. Vertically integrated flux of water vapor for 1200 GCT, 22 July 1961. Lengths of the vectors are proportional to the magnitude of the flux.



Fig. 15. TIROS III satellite cloud observation 1430 GCT, 23 July 1961. (Orbit 161 Frame 17T). Coastlines and zone boundaries are superposed on the cloud picture.

Best Available Copy

The vertical distribution of flux. In Zone One little change in the locations of regions of inflow and outflow had occurred (compare Figures 16 and 12) though the magnitude and depth of the normal flux had decreased by about half. No more is said about this zone as it was not pictured by the satellite.

A stream is shown entering Zone Two (Figure 17) in the vicinity of MIA and NQX. This location was approximately the same as the previous day but the height had increased 150 mb. A more northerly wind component at MID caused the outflow between BRJ and MID to appear larger in area than the previous day. Due to the uncertainty associated with the flux pattern constructed using widely spaced stations, such indications were only rough guides.

The vertically integrated flux. The flux pattern was more distorted again (Figure 18) compared to the flux pattern of the preceding day. The intensity in the western zone decreased appreciably, but with little change in the pattern. The intensity of the flow over MIA and NQX was increased. This increased flow probably curved to the south of MID. Only a slight gradient of flux existed between MID and BRJ.

The largest area of clouds in the northern part of Zone Two existed in a region where the fairly even flow

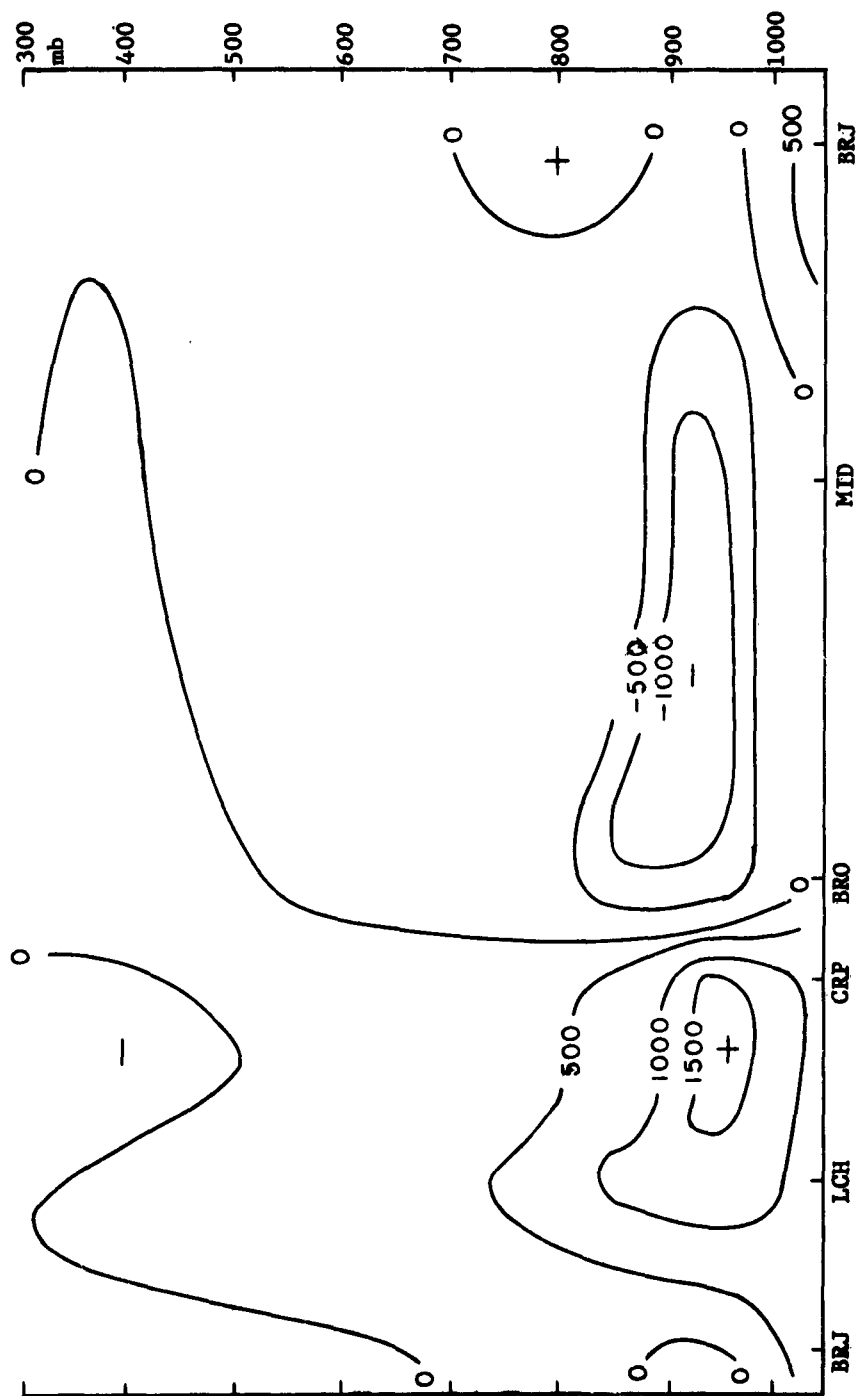


Fig. 16. Vertical distribution of flux of water vapor normal to the base legs of Zone One at 1200 GCT, 23 July 1961. Flux is in  $\text{gm sec}^{-1} \text{m}^{-1} \text{mb}^{-1}$ . Negative flux is inward and positive flux is outward.

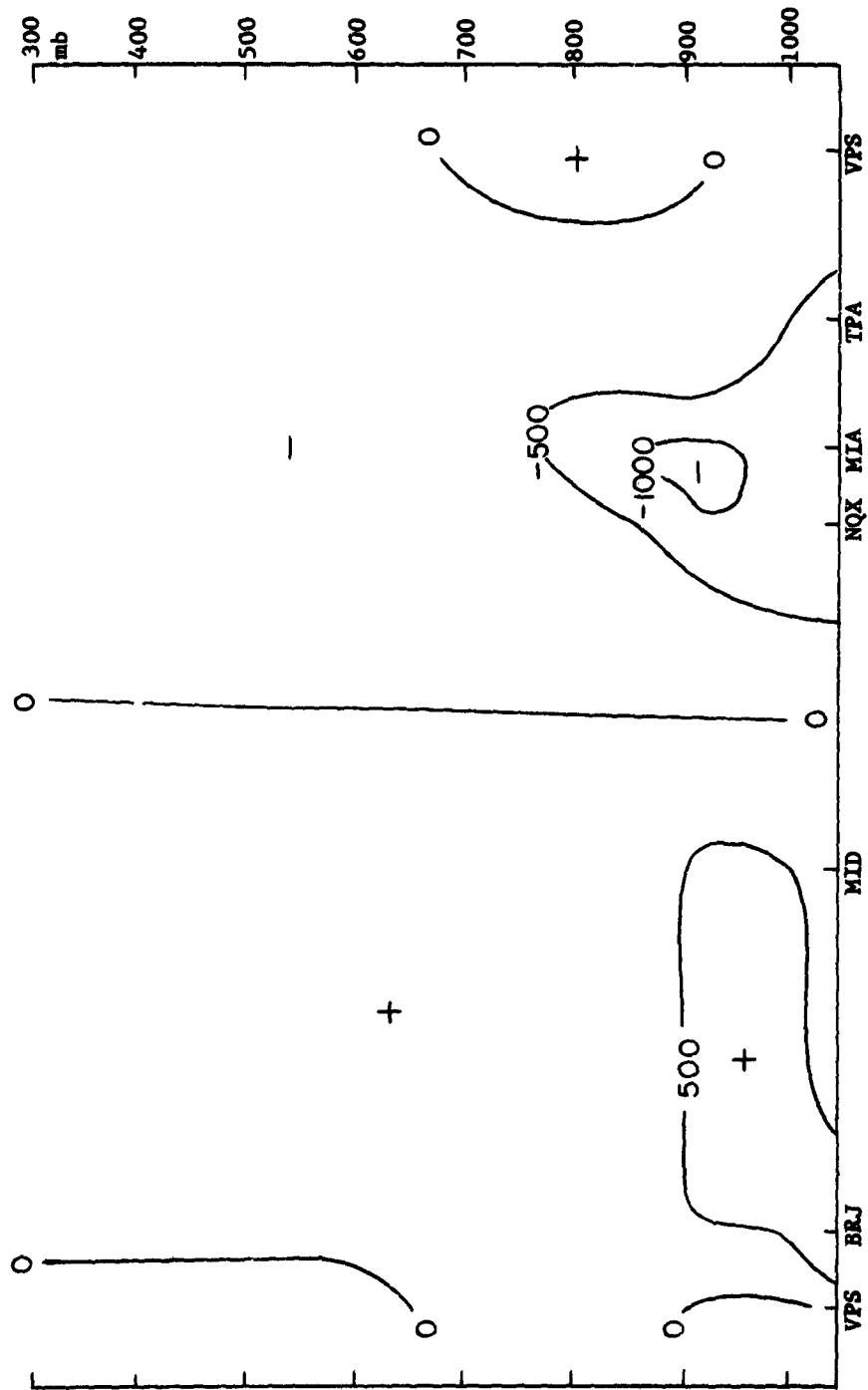


Fig. 17. Vertical distribution of flux of water vapor normal to the base legs of Zone Two at 1200 GCT, 23 July 1961. Flux is in  $\text{gm sec}^{-1}\text{m}^{-1}\text{mb}^{-1}$ . Negative flux is inward and positive flux is outward.

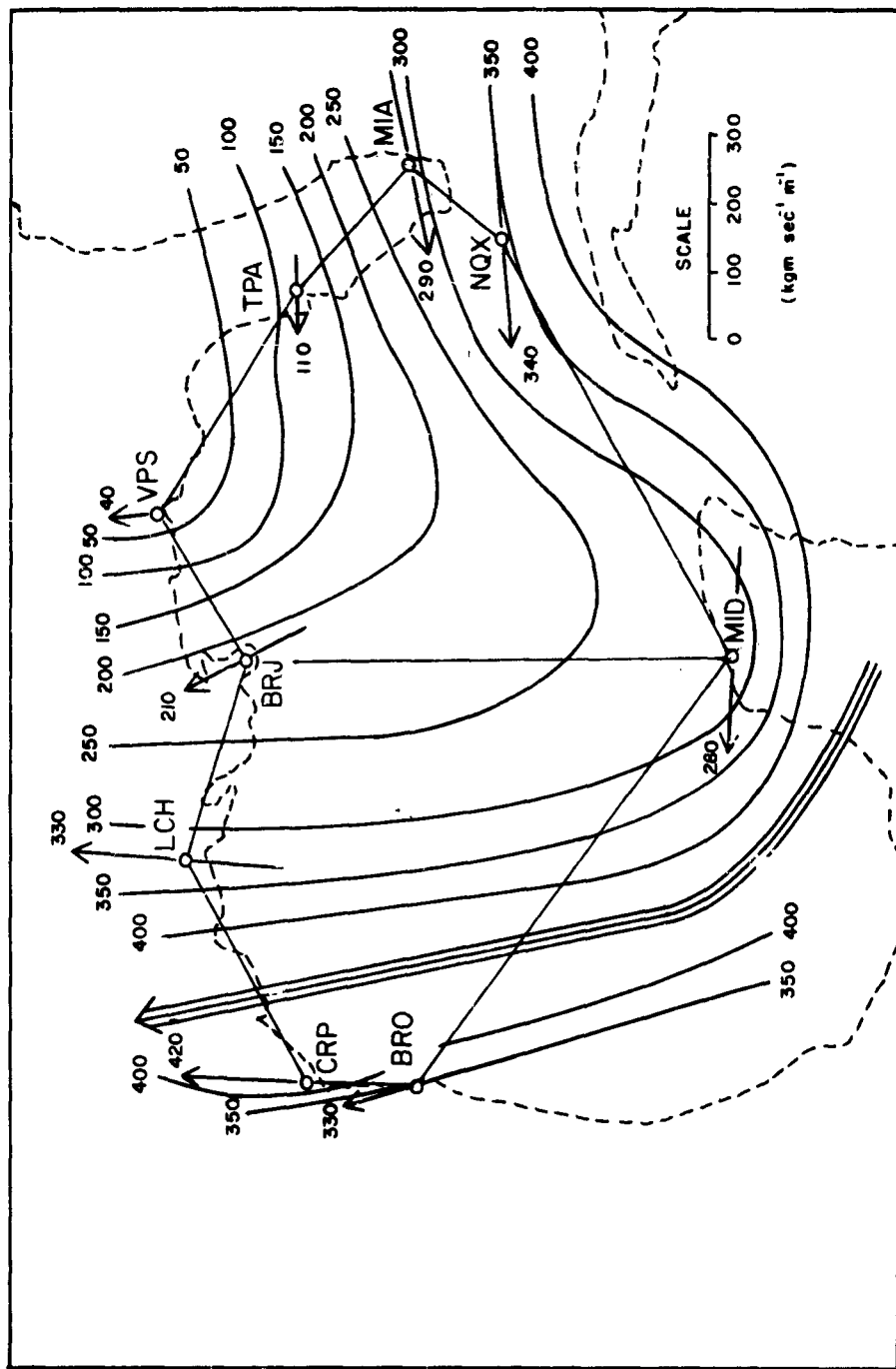


Fig. 18. Vertically integrated flux of water vapor for 1200 GCT, 23 July 1961. Lengths of the vectors are proportional to the magnitude of the flux.

over TPA turned northward into the region between BRJ and VPS. Cloud streaks were present along the southern border of the study area from NQX to MID.

#### Water Vapor Storage, Divergence, Evaporation, and Condensation

The water vapor storage for each zone was measured in cm of precipitable water. This precipitable water storage is presented in Figure 19 for both Zones One and Two. The figure includes the four days under study plus the day preceding the 20th. Although cloud cover over a station was found to increase the computed precipitable water by about 25 per cent, the daily amounts of precipitable water over the zones varies only by about 20 per cent.

The water vapor balance was composed of the rate of change in the precipitable water, water vapor divergence, and the net effect of phase change. This balance was computed from Equation [9] and is illustrated in Figures 20 and 21 for Zones One and Two respectfully.

The water balance for Zone One (Figure 20) suggested an inverse relationship between flux divergence and storage of vapor. When the water vapor was diverging the vapor in storage decreased. Conversely when convergence was taking place the vapor in storage increased. The third day was interesting in that a strong convergence of vapor was more than balanced by a big increase in the amount of

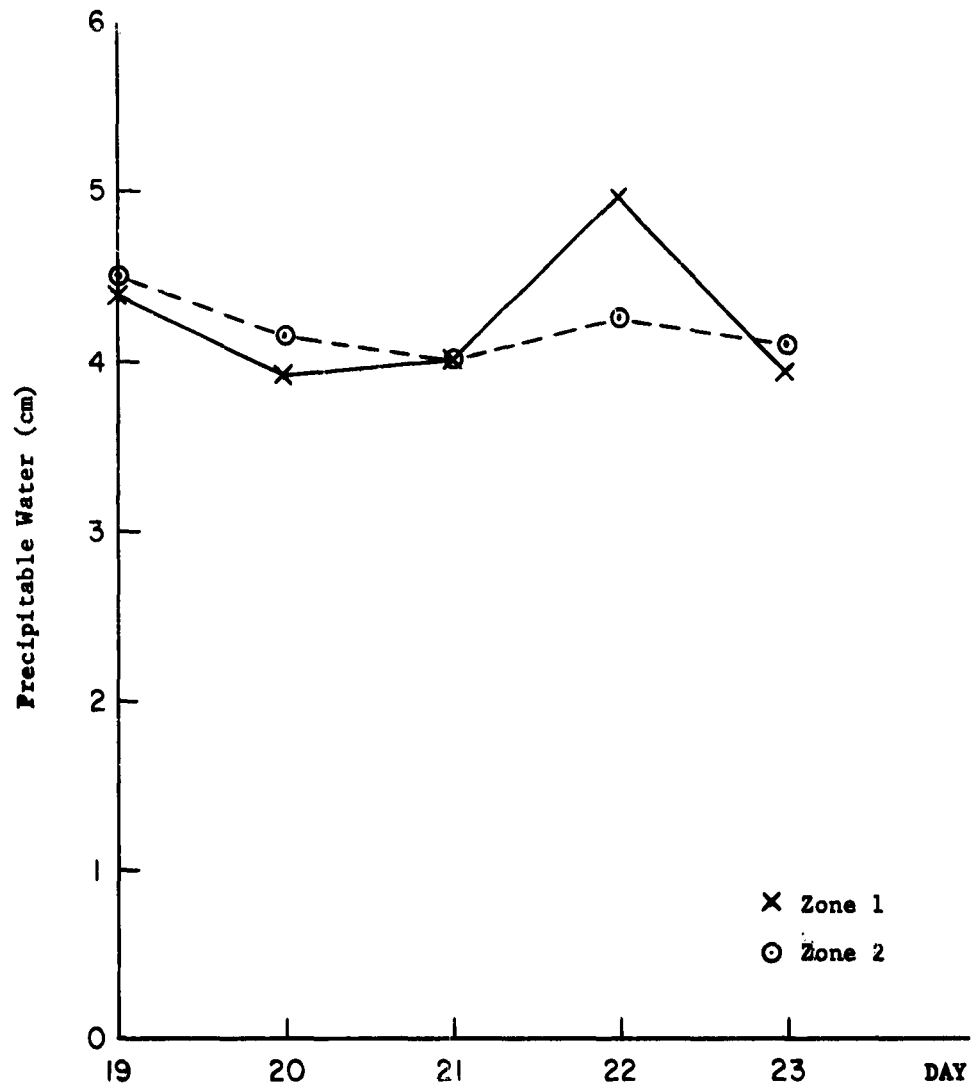


Fig. 19. Precipitable water for Zones One and Two, 1200 GCT, 19-23 July 1961.

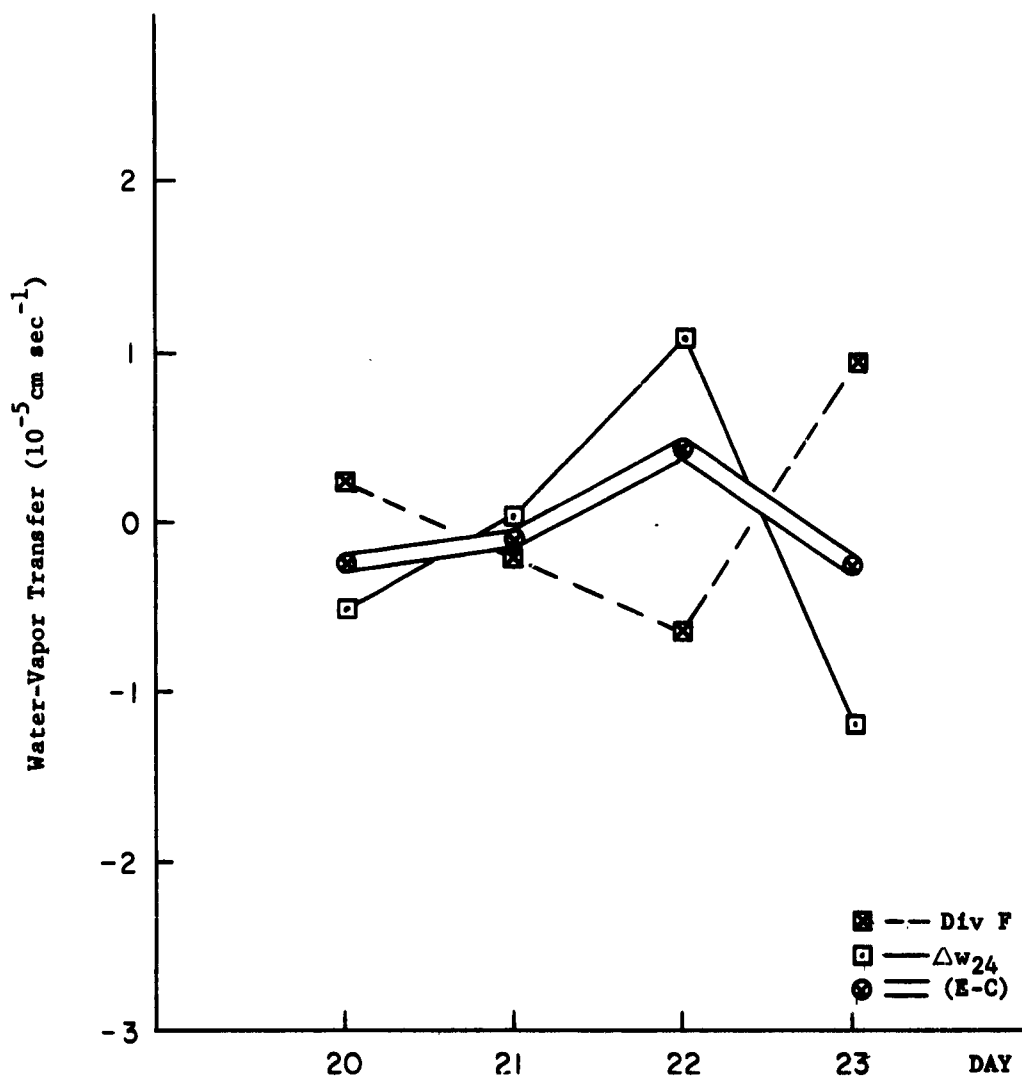


Fig. 20. Water vapor balance for Zone One, 1200 GCT, 20-23 July 1961.  $\Delta w_{24}$  is the rate of change of the water vapor storage for 24 hours.

vapor storage over the zone. The cloud cover for this third day showed no increase, and possibly decreased, compared to that of the previous two days.

The water balance for Zone Two (Figure 21) did not show the same inverse relationship as Zone One. The large convergence occurring on the second day was probably due to a large inflow occurring directly over the measuring stations with the outflow occurring between measuring stations, and therefore going undetected. The third day had the smallest cloud cover, with the vertically integrated flux (Figure 14) indicating a fairly linear distribution of flux for this zone. The indication of evaporation exceeding condensation for this day was considered valid due to the small amount of clouds.

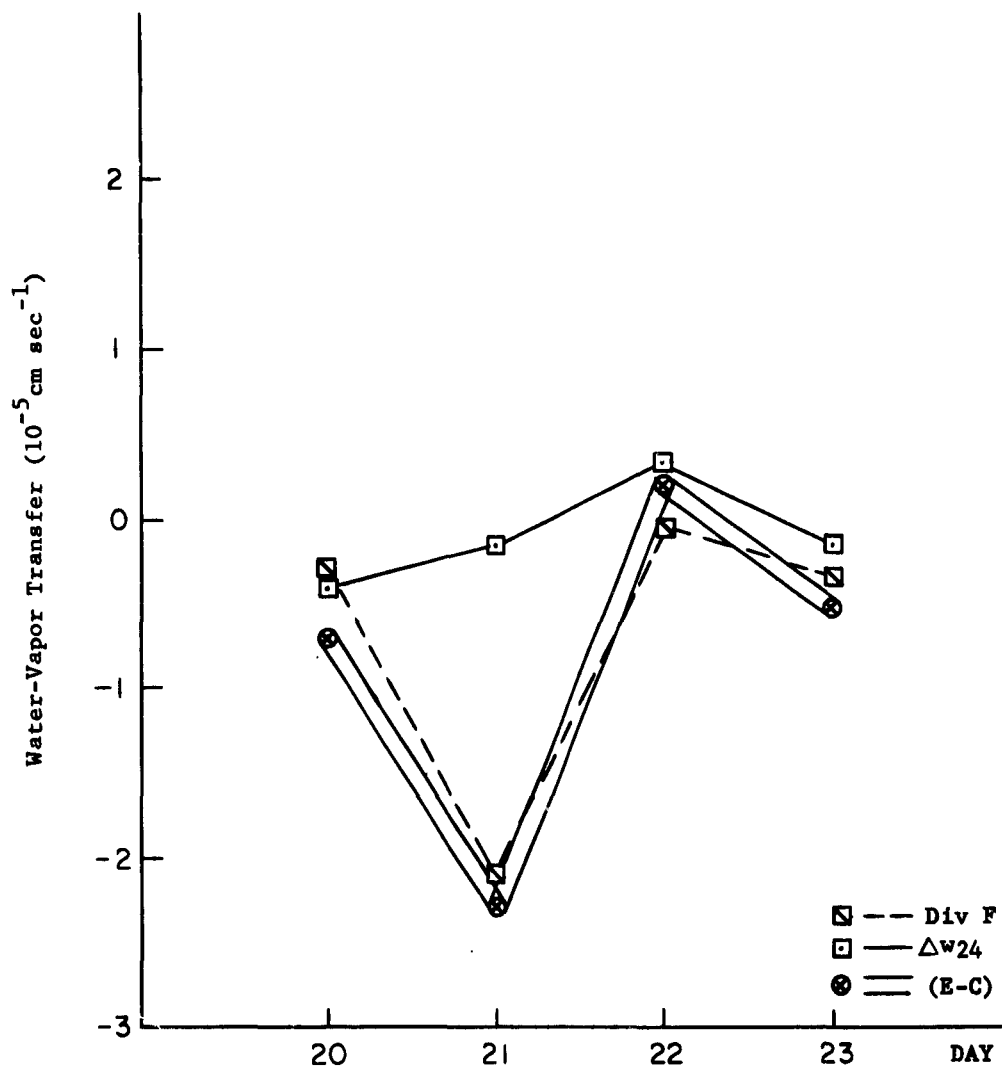


Fig. 21. Water vapor balance for Zone Two, 1200 GCT, 20-23 July 1961.  $\Delta w_{24}$  is the rate of change of the water vapor storage for 24 hours.

## CHAPTER IV

### SUMMARY AND CONCLUSIONS

The illustrations of vertical distribution and vertically integrated values of water vapor flux indicated that the water vapor flow in the volumes tends to resemble stream-type flow. These streams showed considerable temporal variation in width, intensity, height, and location. The main stream may be located outside the zone but its effect on the zone is evidenced by the extension of its high flux values into the zone. During the first day the main cloud areas were located along these streams in the areas of high flux values. The same tendency was present on the other days, but was less pronounced and there were some definite exceptions. Also, clouds seemed to favor a location on the inside of the curve in the flux pattern when the pattern made a definite change in direction. Streaking of clouds appeared to be sometimes associated with these patterns in the areas of higher flux values and stronger gradient. This streaking tended to be parallel to the isolines of flux. The main cloud areas showed a tendency to move in the direction indicated by the vertically integrated flux vectors along the boundary of the zone.

The reliability of the water vapor balance given by

Equation [9] was decreased by the assumption of linear flow between stations. Results of the first day indicated that a strong stream can pass between stations almost undetected. This is due to concentration of high flux values into this stream-type flow. The reliability of the assumption of linear flow is thus dependent upon the distance between stations. As the distance becomes smaller the approximation to the true condition improves.

It is felt that the error caused by the non-linear flow between stations was too great for many conclusions to be drawn from the computations of the water vapor balance. However, some concepts seem valid in spite of this problem. Zone One results indicated a tendency for the water vapor storage to account for the effect of divergence or convergence of water vapor in the volume. Results of Zone One for the third day emphasize the point that convergence of water vapor does not necessarily cause clouds but may just increase the amount of water vapor in storage. The third day in both zones it appeared that evaporation exceeded condensation. This fact is partially verified by the slight decrease in clouds for both zones. The water balance for the first, second, and fourth days generally indicated that condensation was exceeding evaporation. This seems plausible as clouds were present

on these days. Only if clouds had been absent could it have been said that condensation could not exceed evaporation.

The water vapor in storage varied only by about 20 per cent. This constancy may be partly due to the lack of change in the synoptic pattern for the four day period. The air mass over the Gulf was warm and moist and no large-scale modifying factors were present in the local area to change it. The amount of clouds did not show a definite relationship to the precipitable water over the zones. On the third day Zone One had a higher moisture level and no increase in cloud cover.

Further work in this field should prove beneficial. A study of the flux of water vapor in respect to frontal systems and pressure centers should prove fruitful. Any study of clouds should include the water vapor budget to see if the water vapor flux was favorable for cloud formation. Large cloud masses over land could be studied as a single zone if the mass were large enough to cover a group of stations.

In further studies it would be advisable to use a close network of stations, small size zones to more closely approximate the cloud area, and stations inside the zone to detect stream flow. As the method used in this study requires a flat bottom surface for the volume studied, it would be best to restrict study to water

areas or relatively flat terrain. Eventually, the program should be modified to allow use in mountainous areas.

## REFERENCES

- Anonymous, 1955: Accuracies of Radiosonde Data, AWSTR 105-133, Air Weather Service (MATS), USAF, Washington, D. C., 12 pp.
- Benton, G., and Estoque, M., 1953: "An Evaluation of the Water Vapor Balance of the North American Continent," Scientific Report No. 1, 10 pp., John Hopkins University.
- Ellsaesser, Major Hugh W., 1960: Wind Variability, AWSTR 105-2, Air Weather Service (MATS), USAF, Scott AFB, Ill., 84 pp.
- Franceschini, G., 1961: "Hydrologic Balance of the Gulf of Mexico," Unpublished Doctoral Dissertation for Department of Oceanography and Meteorology, A. and M. College of Texas, 50 pp.
- Linsley, R., Kohler, M., and Paulhus, J., 1949: Applied Hydrology, McGraw-Hill, New York, 689 pp.
- McKay, C. M., 1961: "Atmospheric Branch of the Hydrologic Cycle Affecting Texas for Water Year 1959," Unpublished Thesis for Department of Oceanography and Meteorology, A. and M. College of Texas, 50 pp.
- Milne, W., 1953: Numerical Solution of Differential Equations, Wiley, New York, 275 pp.
- Saucier, W., 1955: Principles of Meteorological Analysis, University of Chicago Press, 438 pp.
- Sawyer, J. S., 1962: Performance Requirements of Aerological Instruments, WMO TN 45, World Meteorological Organization, Geneva, Switzerland, 26 pp.
- Starr, V., 1957: "On the Global Balance of Water Vapor and the Hydrology of Deserts," Studies of the Atmospheric General Circulation II, MIT General Circulation Project, pp. 109-123.